

# Study of Shockwave with Supersonic Compressible Flow over an Inclined Flat Plate

Syed Angkan Haider<sup>1</sup>, Shadman Tahmid<sup>2</sup>

<sup>1,2</sup> Department of Mechanical Engineering, Bangladesh University of Engineering and Technology  
<sup>1</sup>angkanhaider@gmail.com, <sup>2</sup>shadmantahmidsuhrid@gmail.com

## Abstract

An inclined flat plate under supersonic compressible flow is analyzed and flow characteristics have been investigated. An angle of attack of 15° is used for the inclined flat plate. Reynolds averaged Navier-Stokes equations with two equation  $k-\omega$  shear stress transport (SST) turbulence model have been applied for the computational analysis. The RANS solver model is used as the RANS equations are time-averaged equations and they can be used to decompose an instantaneous quantity into its time-averaged and fluctuating quantities. With approximations based on knowledge of the properties of flow turbulence time-averaged solutions to Navier-Stokes equations can be obtained. For the supersonic flow, Mach number of 1.5 and 2.0 are used in the investigation. The flow field is investigated and different physical parameters are also studied.

Keywords: Flat plate, RANS model, Supersonic flow, RANS.

## 1. Introduction

The study of flow over an inclined flat plate is and has been an ever-so-important topic as it has widespread applications in the fields of aerodynamics and aerothermodynamics. Breuer *et al.*[1] studied separated flow around a flat plate at an angle of attack of 18° and compared the predictions of the DES, RANS and LES models. The governing equations, modelling approaches, numerical solution methods are given and the results are formulated to give an improved DES formulation. In another study, Knight *et al.*[2] studied the improvements of CFD predictions of shockwave turbulent boundary layer interactions using DNS, RANS and LES models and compared their limitations and capabilities.

Borovoi *et al.* [3] studied the interaction between inclined shock and boundary and high-entropy layers on a flat plate taking into account the presence of the bluntness of the leading edge of the plate. Mach numbers of 6, 8 and 10 were analyzed; 2D Navier-Stokes equations and averaged Reynolds equations using the  $q-\omega$  turbulence model were used. The laminar boundary layer as seen to become turbulent inside the separation zone which the shock induced. At the interference zone, the heat exchange intensity was significantly reduced by the plate bluntness and the effect became more prominent as the Mach number was increased. Nonomura *et al.* [4] analyzed supersonic jets impinging on inclined flat plate and the acoustic waves that were generated; 3D compressible Navier-Stokes equations with a modified weighted compact nonlinear scheme were applied. Acoustic emission and propagation mechanisms were studied and acoustic field characteristics such including directivity, their spectra and the wave source positions. Three different types of acoustic fields were found; nozzle-plate distances and temperatures were also accounted for.

In our study we analyzed shockwave parameters for supersonic compressible flow over an inclined flat plate. Inclined flat plate was at 15°. For our purposes we used Reynolds-averaged Navier-Stokes (RANS) equations; 2-equation  $k-\omega$  shear stress transport (SST) turbulence model was applied. Shock was analyzed at Mach number of 1.5 and 2.0 for the supersonic compressible flow. Different parameters of the flow are investigated.

## 2. Computational Method

### Mathematical Model

The most complete model available for the flow of air is the Navier-Stokes equations. The three conservation laws represented are:

Conservation of mass

$$\frac{\partial(\rho u)}{\partial x} + \frac{\partial(\rho v)}{\partial y} = 0 \quad (1)$$

Conservation of momentum

$$\rho(u \frac{\partial u}{\partial x} + v \frac{\partial u}{\partial y}) = -\frac{\partial \rho}{\partial x} + \mu(\frac{\partial^2 u}{\partial x^2} + \frac{\partial^2 u}{\partial y^2}) \quad (2)$$

$$\rho(u \frac{\partial v}{\partial x} + v \frac{\partial v}{\partial y}) = -\frac{\partial \rho}{\partial x} + \mu(\frac{\partial^2 v}{\partial x^2} + \frac{\partial^2 v}{\partial y^2}) \quad (3)$$

Conservation of energy

$$\frac{\partial(\rho u E)}{\partial x} + \frac{\partial(\rho v E)}{\partial y} = \frac{\partial(\rho u q)}{\partial x} + \frac{\partial(\rho v q)}{\partial y} + \frac{\partial}{\partial x}(u \tau_{xx} + v \tau_{xy}) + \frac{\partial}{\partial y}(u \tau_{xy} + v \tau_{yy}) \quad (4)$$

### Solver Settings

**Table 1.** Solver and viscous models used

Function	Option
Model	<i>k-<math>\omega</math></i> (2 equation)
<i>k-<math>\omega</math></i> model	SST
<i>k-<math>\omega</math></i> option	Compressibility Effects
Turbulent Viscosity	None
Options	None
Solver	Density Based
Space	2D
Gradient Option	Least Squares Cell-Based
Formulation	Implicit
Time	Steady

### 3. Computational Domain

The computational domain was meshed and a user-defined structured mesh was used. The total number of cells used was 78860 for the 2D case. Bias factor was used at different locations in the flow domain for more detailed analysis at the required regions. In the wall normal direction, the first node after the wall was selected in such that the value of wall  $y^+$  was around 1.1. The mesh used is given below along with close-up looks at the places of interest.

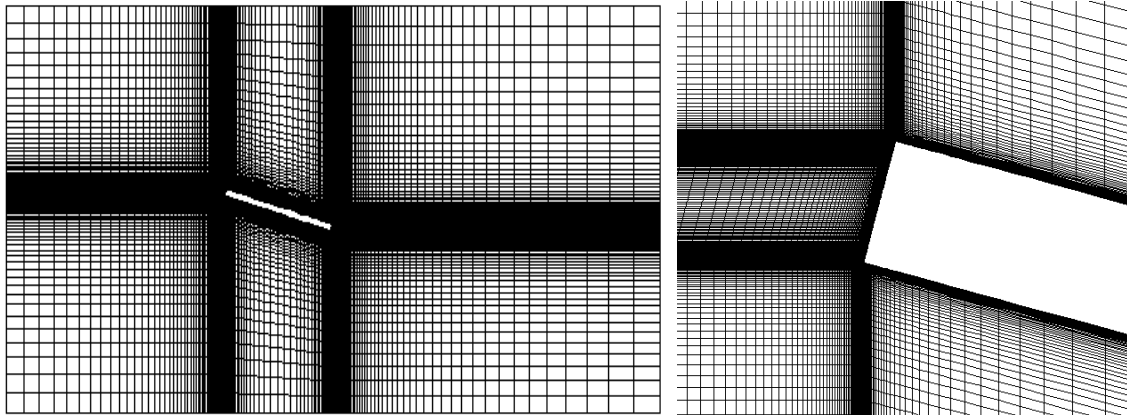


**Fig. 1.** Total discretized domain

Case	Mach Number
------	-------------

Case – 1	1.5
Case – 2	2.0

**Table 2.** Two cases for the experiment

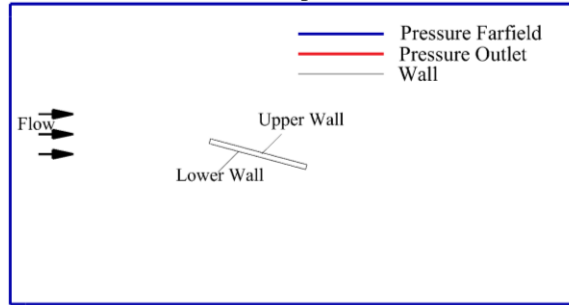


**Fig. 2.** Boundary conditions applied

#### 4. Boundary Conditions

The simulation was conducted with free-stream condition at the farfield with Mach numbers of 1.5 and 2.0. A no-slip adiabatic wall condition was assumed for the wall surface model. Here the flow direction is from the left to the right with a flow angle of  $0^\circ$ .

#### 5. Results and Discussions

Two cases were used for the purpose of our study. The cases were based on two different values of Mach numbers, namely 1.5 and 2.

##### Schlieren Visualization

Numerical schlieren was generated by contour plotting the absolute value of the density gradient. The numerical schlieren did not distinguish between shocks or expansions since absolute value was used.

From the schlieren images, it was observed that for Case 1, a detached shock can be observed, characterized by the high density arc well ahead of the plate leading edge. Attached shock is observed at the plate trailing edge, as seen as four high density lines.

For Case 2, the schlieren image shows a detached shock arc at the plate leading edge like in Case - 1, but much closer to the plate; also four attached shock lines at the plate trailing edge, seen as high density regions on the schlieren images.

##### Total Pressure along walls

The total pressures along the upper and lower walls were plotted and the results for the two cases is given for the upper and lower walls is as given.

For Case -1, the pressure plot for the upper wall shows an abrupt pressure drop at  $x = -0.0042\text{m}$ , but this drop is very short in terms of axial length and the pressure rises again as the flow goes past the leading edge of the plate. The pressure attains a stable value, despite gradually increasing, for most of the flow over the wall afterwards but it rises sharply as the trailing edge is approached at about  $x = +0.0042\text{m}$ .

A flipped result is obtained for the lower wall of the plate; the pressure rises suddenly near the leading edge of the plate at about  $x = -0.0042\text{m}$ . the pressure reaches a maximum value and the remains relatively stable while

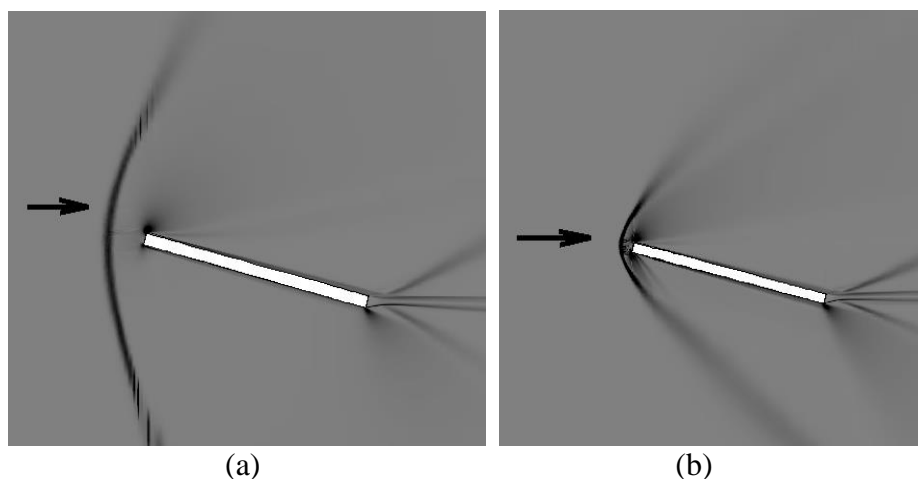


**Fig. 3.** Schlieren image for (a) Case-1 ( $M=1.5$ ) (b) Case-2 ( $M=2$ ).

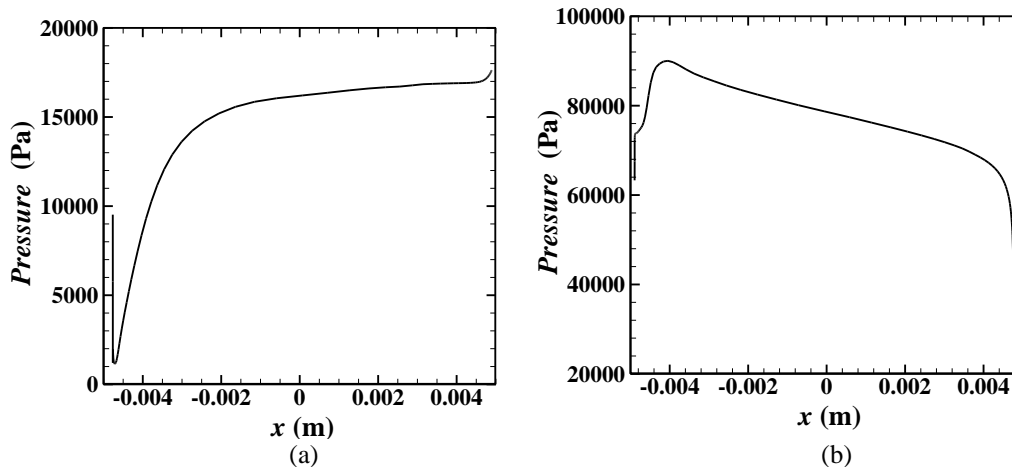


Fig. 4. Pressure plots over the (a) upper and (b) lower walls for  $M=1.5$

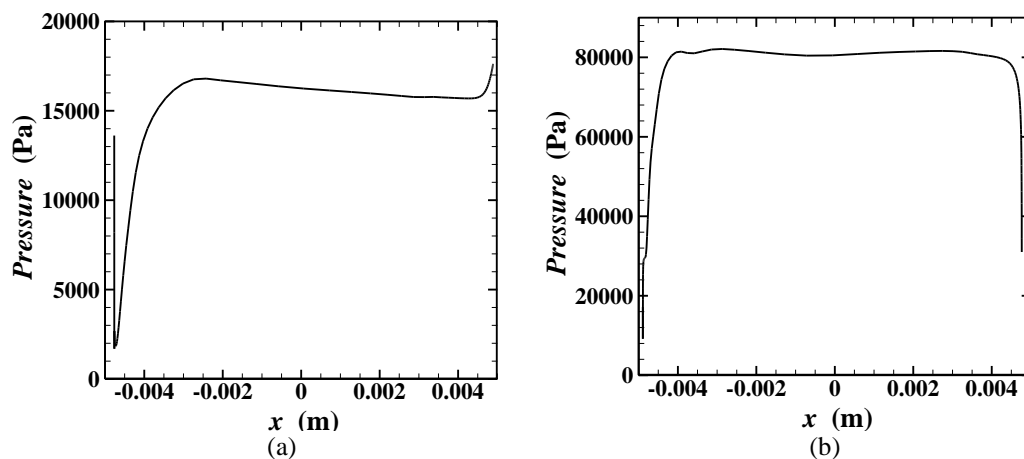


Fig. 5. Pressure plots over the (a) upper and (b) lower walls for  $M=2.0$

decreasing gradually as the trailing edge is approached and decreasing sharply near the trailing edge at about  $x = +0.0042\text{m}$ .

For Case – 2, similar graph as for Case -1 are obtained for the upper wall. However, the pressure drop is even sharper for this higher Mach number flow in terms of axial length and takes place at around  $x = -0.0042$ . Also, after reaching a maximum value, the pressure maintains a stable value while gradually decreasing along the length of the plate as opposed to the increasing pressure for Case -1. As the trailing edge is approached, the pressure again rises sharply at about  $x = +0.0042\text{m}$  like the lower Mach number case.

The graph of pressure for the lower wall for Case – 2 is different from that of the lower Mach number flow in the sense that for this case, the pressure rises sharply at about  $x = -0.0042\text{m}$  and the remains constant for the remaining of the plate, as seen by the plateau formed, before approaching the trailing end of the plate, where the pressure plummets abruptly at around  $x = +0.0042\text{m}$ .

### Pressure Contours

Shockwaves cause a rise in static pressure and expansions cause a drop. Both of these phenomena are visible from the contours.

### Wall Shear Stress Distribution

The wall shear stress plots ( $x$ -wall shear plots) give an indication of flow separation in the wall. A negative value of  $x$ -wall shear stress means flow separation.

From the plots, it can be seen that the shapes of the curves for the upper and lower walls for the different Mach number cases are quite similar. It can be seen that for the upper wall, the pressure plummets from a very high value abruptly to a value of wall shear at below 0 or close and the rises above 0 ever so slightly and stays

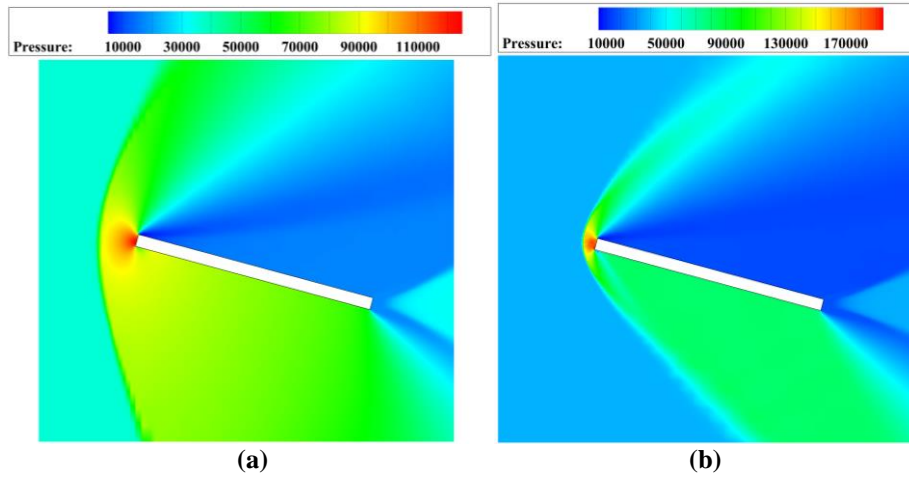


Fig. 6. Pressure contour for (a) Case-1 (M=1.5) and (b) Case-2 (M=2.0).

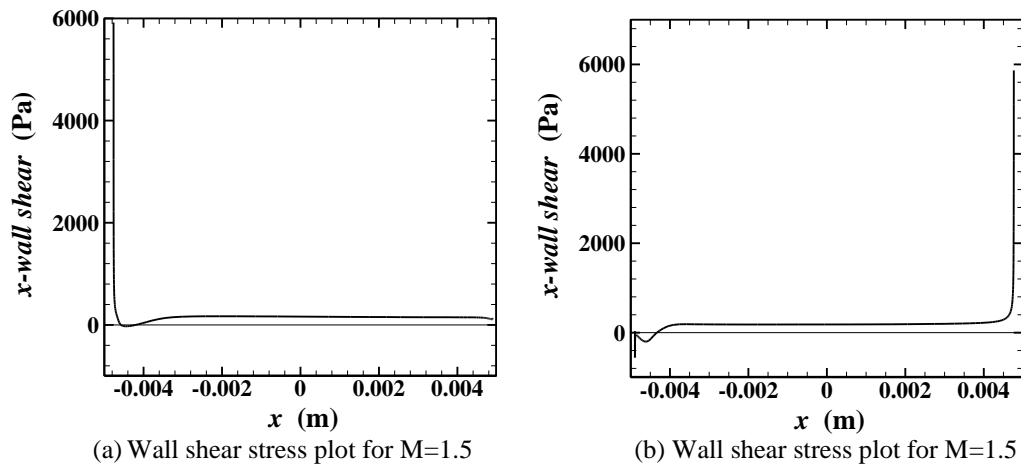


Fig. 7. Wall shear stress plots for upper and lower walls for M=1.5

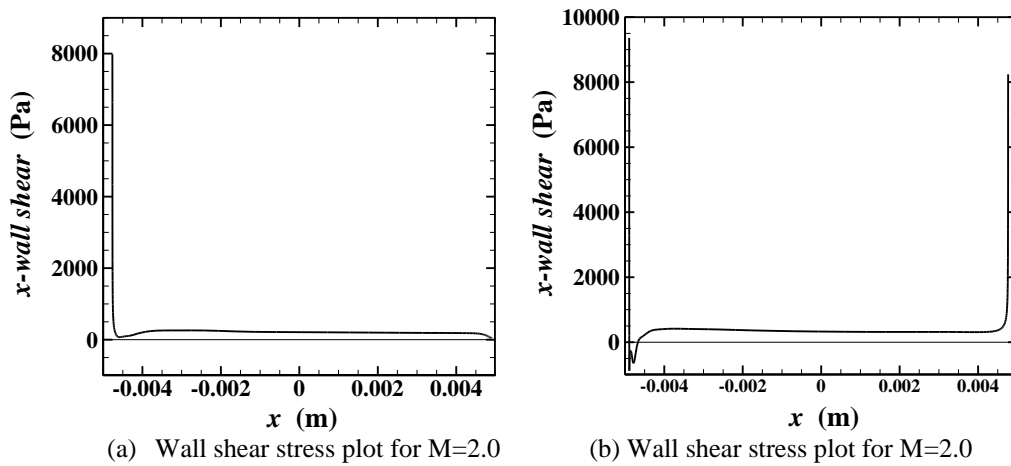


Fig. 8. Wall shear stress plots for upper and lower wall for M=2.0

constant along the plate as seen by the flat shape of the curve. The notable thing from the plots of the upper wall shear stress for the two different M number values is the fact that the minimum values of shear stress occurs at about  $x = -0.0043\text{m}$  but for  $M = 1.5$ , the minimum value is less than 0 for a small region, a clear indication of flow separation near the leading edge of the plate. But for the M value of 2.0, the minimum value occurs above 0 and so no flow separation occurs at this Mach number at the upper wall.

For the lower, the graphs are similar. At  $M=2.0$  wall shear stress remains below 0 for  $x < -0.0042$  and this is an indication of flow separation. After this region, the shear stress increases above 0 and remains constant above this value before rising sharply at about  $x = +0.0042\text{m}$  near the trailing edge of the plate. For  $M=2.0$ , the shear stress plummets from a high value to below zero sharply, remains below zero for a small region before again rising just above 0 and remaining constant for the rest of the plate, until the trailing edge is approached, where, at about  $x = +0.0042\text{m}$ , the shear stress increases sharply.

## 6. Conclusion

Shock at the leading edge was observed to be detached for both  $M=1.5$  and  $M=2.0$ , but for  $M=2.0$ , the shock was much closer to the plate than for  $M=1.5$ . As for the plate trailing edge, shock was attached for both cases. Pressure variations for the upper and lower walls were quite similar for the two cases. But for overall flow much greater pressures were observed for the second case. The wall shear stress plots show that flow separation takes place for  $M=1.5$  but for the higher M flow is not separated.

## 7. Acknowledgement

This research was supported by the members of the research group Multiscale Mechanical Modelling and Research Network (MMMRN), BUET and we are indebted to all of them.

We would like to thank Md. Shahriar, Dept. of ME, BUET, for imparting some of his skill regarding the software used.

## 8. References

- [1] Breuer, M., Jovičić, N. and Mazaev, K., "Comparison of DES, RANS and LES for the separated flow around a flat plate at high incidence". *International journal for numerical methods in fluids*, 41(4), pp.357-388, 2003.
- [2] Knight, D., Yan, H., Panaras, A.G. and Zheltovodov, A., "Advances in CFD prediction of shock wave turbulent boundary layer interactions". *Progress in Aerospace Sciences*, 39(2), pp.121-184, 2003.
- [3] Borovoi, V.Y., Egorov, I.V., Skuratov, A.S. and Struminskaya, I.V., "Interaction between an inclined shock and boundary and high-entropy layers on a flat plate". *Fluid Dynamics*, 40(6), pp.911-928, 2005.
- [4] Nonomura, T., Goto, Y. and Fujii, K., "Aeroacoustic waves generated from a supersonic jet impinging on an inclined flat plate". *International Journal of Aeroacoustics*, 10(4), pp.401-425, 2011.